# AUTOMATIC CONTINUOUS TRANSVERSE BEAM-SIZE MEASUREMENT SYSTEM FOR KEKB

J.W. Flanagan, S. Hiramatsu, and T. Mitsuhashi
High Energy Accelerator Research Organization (KEK)
1-1 Oho, Tsukuba-shi, Ibaraki 305-0801, Japan

*Abstract*

In order to measure beam sizes at KEKB, we have installed synchrotron radiation (SR) monitors in each of the electron and positron storage rings, capable of both direct imaging and SR interferometry measurements. The interference pattern from the SR interferometer is digitized and analyzed using a non-linear fit for precise beam-size measurements in both the horizontal and vertical transverse planes. The results are relayed back to the control room for continuous real-time monitoring of the beam-sizes, which has proven useful for collision tuning and general beam studies. We here report on the data acquisition and analysis system.

## 1 INTRODUCTION

Each of KEK B-Factory's two storage rings, the HER and the LER, has a complete, independent SR monitor system, consisting of a 5 mradian bend SR source magnet, water-cooled beryllium extraction mirror, closed optical beamlines and above-ground optics hutch.[1] Each beamline transports the SR beam 30-40 meters to an external optics hutch along two parallel paths. One path is designed for direct imaging with adaptive optics[2], the other is used for transverse beam size measurements via SR interferometer[4], as well as streak camera and high-speed gated camera measurements[3].

The focused image and the interference pattern are captured with CCD cameras in the optics hutch. The interference pattern is analyzed by image processing software running on a computer in the hut to extract the visibility of the interference fringes. This information, along with the images themselves, is transferred to an EPICS IOC host, where the beam size is calculated from the visibility. The automated system is described here.

## 2 INTERFERENCE PATTERN ANALYSIS

The geometry of interference pattern formation is as shown in Figure 1. The SR light from the beam comes into each slit with an intensity $I$, assumed (and adjusted) to be equal in magnitude for each slit. The two slits have width $w$ and are separated by a distance $D$, with the interference pattern being formed a distance $F$ from the slits.

For a single-wavelength component of the incident SR, the interference pattern produced has an intensity distribution $y(x)$ of the form

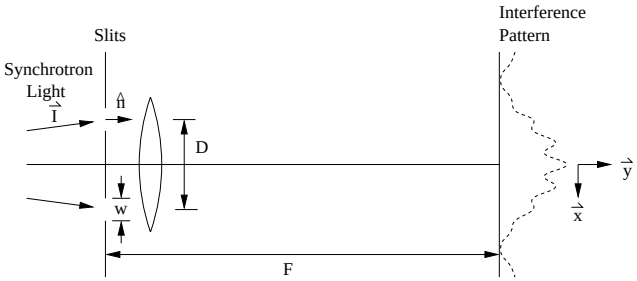


Figure 1: Geometry of interference pattern formation.

$$y(x) = I_0 \left[ \frac{sin(\frac{2\pi}{\lambda} F w \Phi x)}{\frac{2\pi}{\lambda} F w \Phi x} \right]^2 (1 + \gamma cos(\frac{2\pi}{\lambda} D x)), \quad (1)$$

where $I_0 \propto |\vec{I}|$ is determined by the intensity of the beam, $\lambda$ is the wavelength of the light, and $\Phi \propto \vec{I} \cdot \hat{n}$ is an effective slit width correction. This represents two single-slit diffraction patterns $(sin(x)/x)^2$ brought into overlap by the lens behind the slits, modulated by a cosine double-slit term with visibility $\gamma$ determined by the spatial coherence of the SR light. The visibility is the desired quantity, from which the beam size is calculated, assuming a gaussian beam distribution and negligible source depth effects, as

$$\sigma_{beam} = \frac{\lambda L}{\pi D M} \sqrt{\frac{1}{2} \ln \frac{1}{\gamma}}, \quad (2)$$

where $L$ is the distance from the beam source point and $M$ is the magnification of the optical path due to curvature in the extraction mirror.

## 3 FUNCTIONAL FIT

To find the visibility $\gamma$ from the interference pattern, we fit the measured pattern using the standard Levenberg-Marquardt method for non-linear fitting.[5] For this purpose, we introduce some additional terms to Equation 1 to represent a linear background, and also to correct for offsets in the origin of the image axis $x$, which can change as the image moves due to air fluctuations or changes in the beam orbit. Separate offsets are needed for the $sinc$ and $cos$ terms because small offsets in the path length to each slit from the beam will move the origin of the $cos$ pattern relative to that of the $sinc$ pattern. In addition, since the size of the interference pattern is adjusted using additional

lenses between the slits and the CCD (not shown in Figure 1), the scales of the $sinc$ and $cos$ terms are taken initially as parameters.

For maximum light intensity while measuring beam sizes at low beam currents, we use bandpass filters with a fairly large FWHM of 87 nm around a center wavelength of 513 nm (Melles Griot 03 FIB 006). The effect of such a large bandwidth is to smear the monochromatic interference pattern of Equation 1 progressively as one observes from the center of the pattern towards the edges, due to the overlapping of patterns at different characteristic scales (wavelengths). To account for this we write the fitting function as a sum over a sample of wavelengths covered by the filter, each term weighted by the transmission at that wavelength, as shown in Figure 2. The incident SR spectrum changes by only a few percent over this bandwidth, and is taken as flat.

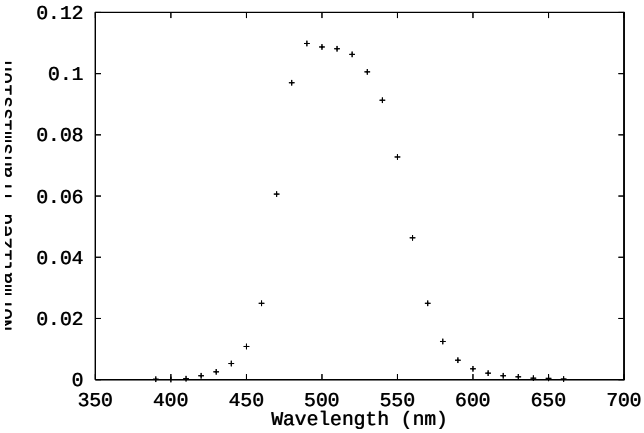


Figure 2: Light transmission curve of SR interferometer bandpass filter. Integral under the curve is normalized to unity.

The inputs are thus the fitting function,

$$y = a_1 + a_2 x + \sum_{i=1}^{n} f_i \frac{a_3}{2} \left[ \frac{sin(\frac{\lambda_0}{\lambda_i} a_4 (x - a_5))}{\frac{\lambda_0}{\lambda_i} a_4 (x - a_5)} \right]^2 \times (1 + a_6^{(\lambda_0/\lambda_i)^2} cos(\frac{\lambda_0}{\lambda_i} a_7 (x - a_8))),$$

and its partial derivatives $\partial y / \partial a_i$. In the above equation, $n$ is the number of wavelengths $\lambda_i$ over which the filter response function $f_i$ (with central wavelength $\lambda_0$) is sampled. Parameter $a_6$ is the visibility $\gamma$ of Equation 1; the exponent appearing on this parameter here represents the variation of visibility observed at different wavelengths relative to that observed at the central wavelength, assuming a Gaussian beam with the same apparent beam size at all wavelengths (i.e., using Equation 2). For the monochromatic case this exponent is of course unity and so does not appear in Equation 1.

The interference pattern is digitized from CCD camera images and analyzed using a commercial image analysis package (WiT), which provides hooks for user-developed routines to be included, where we have installed the above procedure. Before fitting, a vertical smoothing filter is run over the image to reduce noise, and then the peak horizontal row is extracted. The interference pattern $x$ axis goes along the horizontal axis in the images shown here. The vertical beam size is measured by rotating the SR light 90 degrees before reaching the slits.

Figure 3 shows the screen of the image processing computer in the optics hutch.

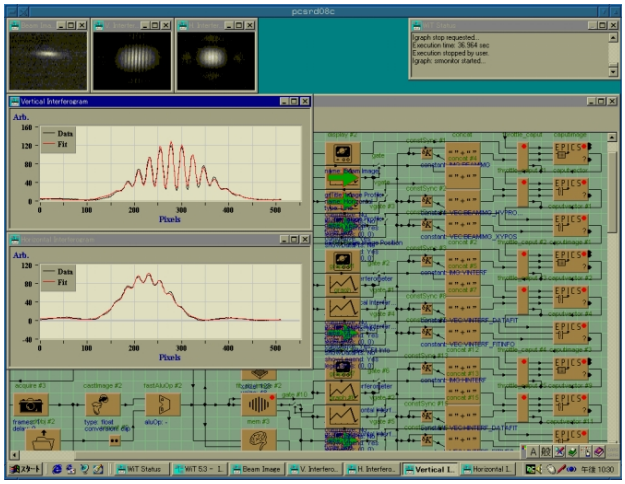

Figure 3: Screenshot of image-processing computer in LER optics hut during image acquisition and analysis.

The fit results are sent to an EPICS IOC host, which calculates the beam size at the SR source bend and maps the result to the interaction point via the beta functions. Figure 4 shows the display panel in the control room.

## 4 PERFORMANCE

The system operates at a continuous repetition rate of about 2 Hz, which is a 20-fold increase over the update rate of 2 months ago, achieved by software improvements and the purchase of faster computers for the data acquisition and fitting. The high update rate was needed for the iSize feedback[6], which adjusts the ratio between the LER and HER beam sizes to maximize the luminosity. An even higher-speed mode has also been implemented which takes data at 60 Hz for a few minutes at a time, then fits the data offline in order to measure the spectra of beam size and position fluctuations.

In general the system works well, but several issues remain. The optical axis needs continual adjustment to correct for slow beam orbit drifts, and also for changes in the optical axis due to heating and cooling of the extraction mirror chambers over the course of a fill. A software feedback system using remotely controllable mirrors in the optical beamline is being implemented to handle this chore.

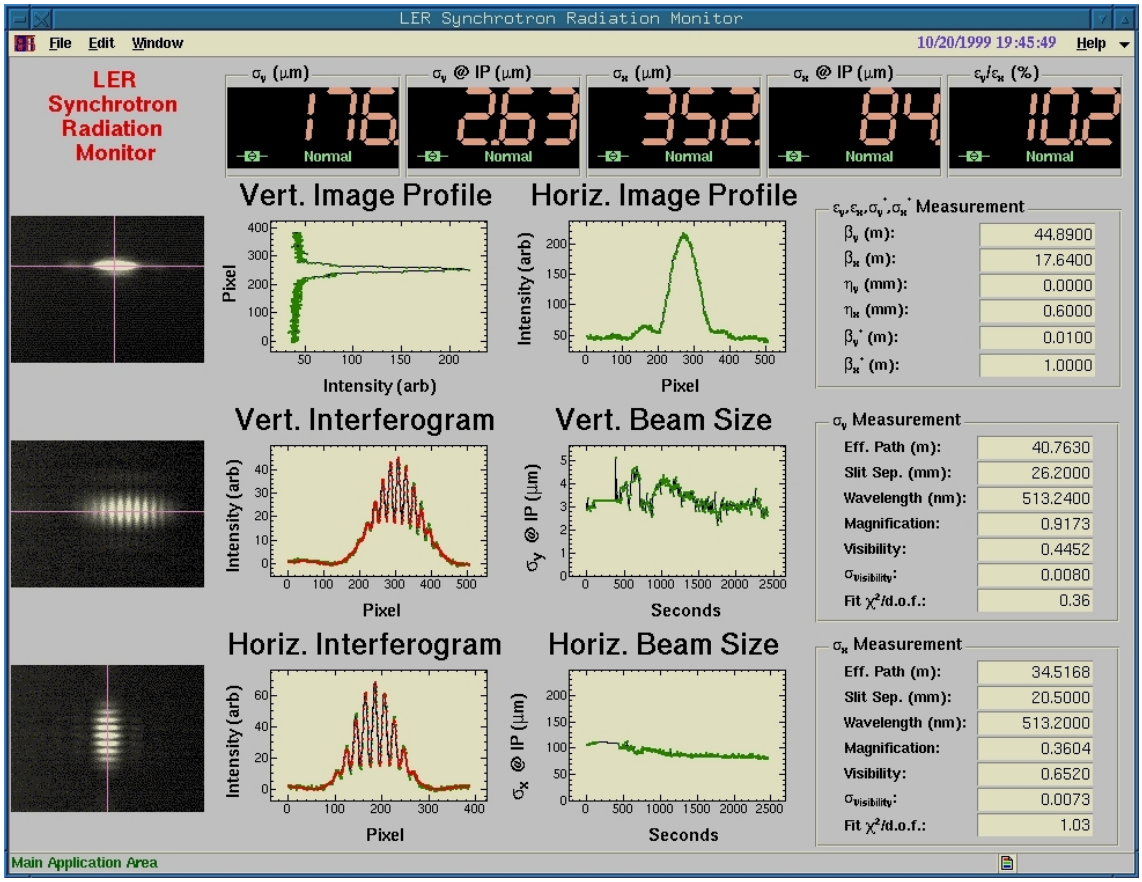


Figure 4: SR Monitor beam-size monitoring panel in control room, showing LER vertical beam size. A companion panel shows the HER beam size.

The mirror surfaces are gradually developing dark bands in the middle where the most intense radiation strikes. The light balance between the two slits periodically needs adjustment due to variations in mirror reflectivity. A set of movable shutters is being installed to make automated measurements of the light balance, from which the correction factor to the visibility can be calculated. In addition, the mirrors will be serviced during the coming summer shutdown.

## 5 CONCLUSION

The online SR interferometry analysis system for the KEKB LER and HER is working well to deliver continuous, real-time measurement of the beam size via SR interferometry. Further automation of the fine-tuning components is underway.

## 6 ACKNOWLEDGMENT

The authors are indebted to the KEKB commissioning team for their continued support and patience, and to the support of Prof. S. Kurokawa for the construction and commissioning of the SR monitoring system and of KEKB.

## REFERENCES

[1] T. Mitsuhashi, J.W. Flanagan, and S. Hiramatsu, "Optical Diagnostic System for KEKB B-Factory," these proceedings.

[2] N. Takeuchi et al., Tech. Digest of Nonastronomical Adaptive Optics (NAAO'97), (1997) p. 26.

[3] J.W. Flanagan et al., "High-Speed Gated Camera Observations of Transverse Beam Size Along Bunch Train at the KEKB B-Factory," these proceedings.

[4] T. Mitsuhashi et al., Proc. EPAC 1998, p. 1565.

[5] W.H. Press, S.A. Teukolsky, W.T. Vetterling and B.P. Flannery, *Numerical Recipes in C: The Art of Scientific Computing*, Second Edition, CUP (1992) pp. 681-688.

[6] N. Iida et al., these proceedings.